Electronic Supplementary Material (ESI) for ChemComm.

SUPPORTING INFORMATION

Efficient photoluminescence of isotropic rare-earth oxychloride nanocrystals from a solvothermal route

Guillaume Gouget,[a] Morgane Pellerin,[b] Lauriane Pautrot-D'Alençon,[b] Thierry Le Mercier,[b] and Christopher B. Murray*[,a]

[a]Department of Chemistry, University of Pennsylvania, Philadelphia, Pennsylvania 19104, United States
[b]Solvay, Research and Innovation Center Paris, F-93308, Aubervilliers, France

EXPERIMENTAL SECTION

Chemicals. Heptahydrated lanthanum trichloride (GFS Chemicals, 99.9 %), hexahydrated europium trichloride (GFS Chemicals, 99.9 %), oleylamine (OLA, Sigma-Aldrich, 70 %), oleic acid (OA, Aldrich, 90 %), methanol (MeOH), toluene and chloroform (Fisher, ACS grade) were stored in air prior to use.

Synthesis of LaOCl nanocrystals. Hydrated RE chlorides in various proportions (0.5 mmol total RE molar content) were dissolved in MeOH (10 mL) prior to addition of OLA (20 mL) in air, at RT. MeOH was evaporated and the mixture was then degassed 1 h at 120°C and 1 Torr. The temperature was increased to 220 °C in 13 min under N_2. After 1 h at 220 °C, OA (5 mL) was injected to the mixture, the temperature suddenly dropped to 200 °C, and then reactant medium was further cooled down to RT by blowing cool air on the vessel. 10 mL of toluene was added, then 10 mL of MeOH. The precipitation of a white solid was observed. The precipitate was centrifuged at 8900 g during 3 min, the supernatant was discarded and a white pellet was recovered. The pellet was redispersed in 10 mL of toluene, and then the dispersion was reprecipitated with 15 mL of MeOH. After purification, the pellet was redispersed in chloroform.

Structural characterization. Powder X-ray diffraction (XRD) diagrams were acquired on a Rigaku Smartlab diffractometer with Cu Kα radiation (λ =1.5416 Å, 40 mA and 30 kV) and parallel beam setting in the θ-2θ geometry. 2θ range was screened between 10 and 80 ° with 0.05° (2θ) steps and during 35 s per step. Peak identification was performed using the cif files from the crystallographic open database (COD), collection code 9009170 (LaOCl) and the inorganic crystal structure database (ICSD), collection codes 77820 (GdOCl) and 84336 (LaOBr)). Apparent crystal size ε_{hkl} were calculated using the Scherrer formula:

$$\beta = \beta_{cris} = \frac{\lambda}{\varepsilon_{hkl} \cos\theta} \qquad (1)$$

β is the integral width of the peak, λ is the X-ray source wavelength and ϑ is the incident beam angle. β was calculated for each separate experimental peak (hkl) by fitting it with a pseudo-Voigt function, using the WinPLOTR function (FullProfSuite).[1] ε was then averaged from all values calculated on a single diagram.

Energy dispersive spectroscopy (EDS) was performed on a JEOL 7500F high resolution scanning electron microscope equipped with an EDS detector. Acceleration tension of the source was 10 kV. RE/Cl atomic ratio was calculated from the average of EDS spectra measured on three distinct 100 x 50 µm^2 areas of aggregated particles. Data were analyzed using the INCA software (Oxford). The sample was dropcasted on a Si wafer, followed by drying, before a carbon layer was sputtered.

Inductive coupled plasma-optical emission spectrometry (ICP-OES) was performed on a Spectro Genesis spectrometer with a concentric nebulizer. Calibrated solution of La and Eu were purchased from Inorganic Ventures. Solid samples were dissolved in HNO_3 (70 $\%_{mas.}$) at 60 °C.

Transmission electron microscopy (TEM) images of NCs were collected on a JEOL JEM-1400 microscope operating at 120 keV. Samples were prepared by depositing a drop of NCs in chloroform (3.10^{-2} g.L^{-1}) on a carbon-coated copper grid. Selected area electron diffraction (SAED) was performed

with a camera distance of 20 cm. Interreticular planes were deduced from distances calibrated with a known sample of silicon particles. Size distribution data were extracted from at least 100 particles on pictures taken on at least 3 distinct regions of a TEM grid.

Optical characterization. Absorption spectra of the dispersions were measured in a 10 mm quartz cuvette, on a Cary 5000 UV−vis−NIR spectrophotometer (Agilent Technologies) from 800 to 200 nm with a 1 nm step. The same cuvette filled with solvent was used as a reference.[2-5] **Photoluminescence** (PL) experiments were performed on a FLS1000 fluorimeter (Edinburgh Instruments) equipped with a Xe lamp and a PMT detector. PL spectrum was acquired from 310 to 800 nm with 1 nm steps and 0.1 s per step. Slit bandwidths on both incident and emission sides were 1.1 nm. PL excitation spectrum was acquired from 270 to 610 nm, 1 nm steps and 0.1 s per step. Slit bandwidths on both incident and emission sides were 2.0 nm. PL decay measurements were performed with a pulsed laser source (MCS) at 378 nm, 125 Hz pulse frequency. For absolute PL quantum yield measurement, an integrating sphere was adapted on the fluorimeter. Emission spectra were acquired in the same condition for the reference (cuvette with solvent) and sample with an optical density of 0.1: λ_{exc} = 300 nm (or 395 nm), 10 nm slit bandwidth on the incident side, 1.0 nm slit bandwidth on the emission side, 270 (or 370) to 800 nm, 1 nm steps and 0.5 s per step.

ADDITIONAL DATA

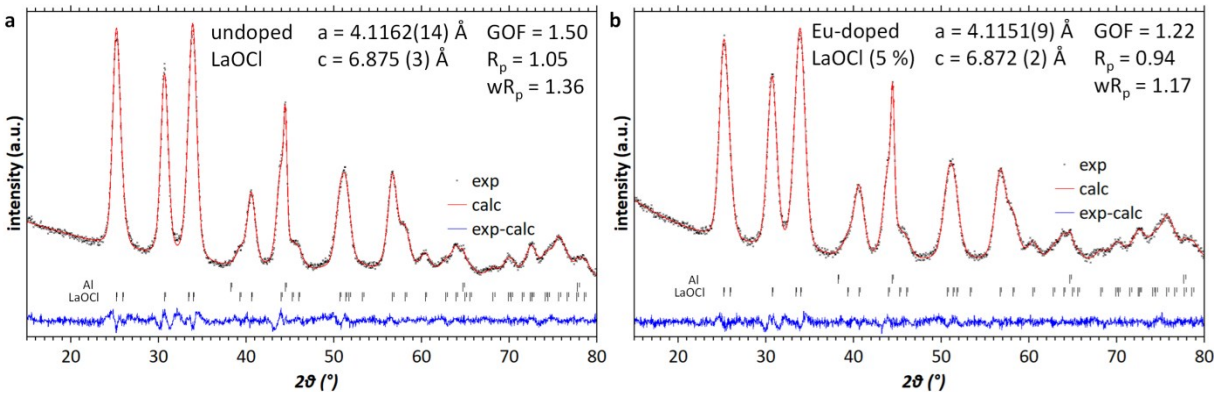

Figure S1. Le Bail refinements of a) undoped and b) 5 % Eu^{3+}-doped LaOCl nanocrystals. The peak at 2θ = 44.5 ° is due to the aluminum plate. It is taken into account in the fit (Al, Fm-3m, ICSD .cif file code 64700) in the refinements. In both cases, refined cell parameters of LaOCl (P4/nmm) are similar to values reported (COD .cif file 9009170): a = 4.119 Å and c = 6.883 Å. Refinements were performed on JANA 2006.[6]

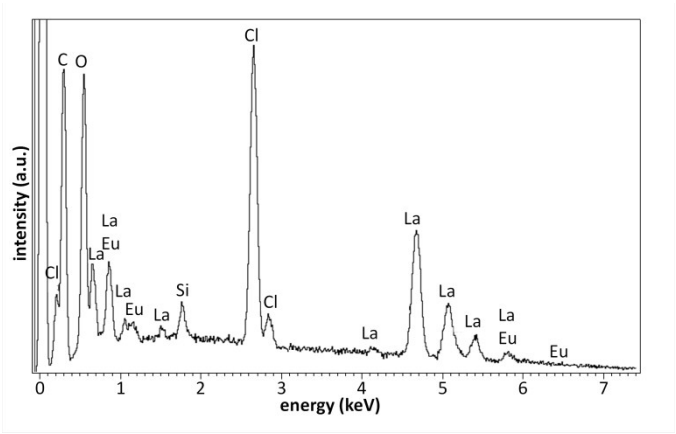

Figure S2. SEM-EDS spectrum of a region of aggregated Eu^{3+}-doped LaOCl NCs. Si detection is attributed to a contamination from sample preparation or SEM chamber. It is not considered for quantification, nor O and C.

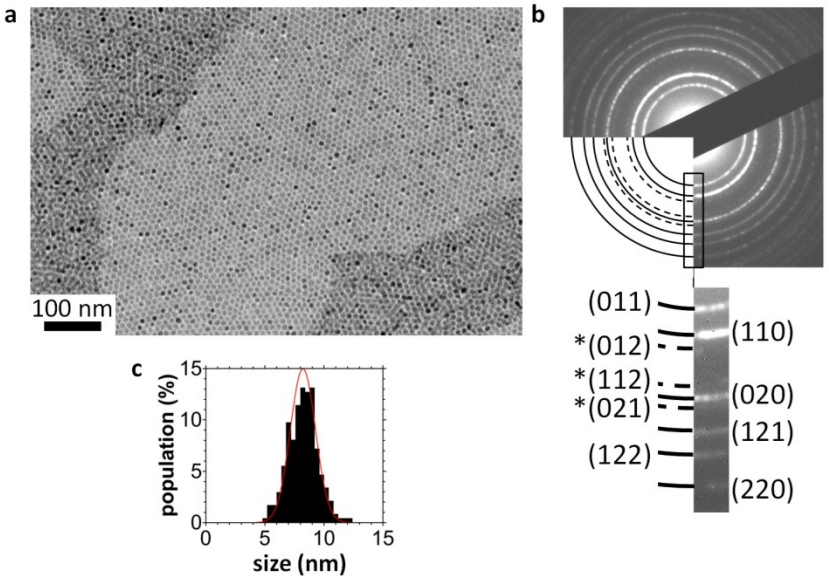

Figure S3. a) TEM picture of 5 % Eu^{3+}-doped LaOCl nanocrystals forming close-packed monolayers and bilayers. b) SAED picture with diffraction rings indexed along with LaOCl structure. Lower left inset is a scheme reproducing (full lines) major and *(dashed) minor rings. c) Size distribution diagram of 5 % Eu^{3+}-doped LaOCl nanocrystals (black) and gaussian function centered at 8.2 nm with a 1.1 nm standard deviation.

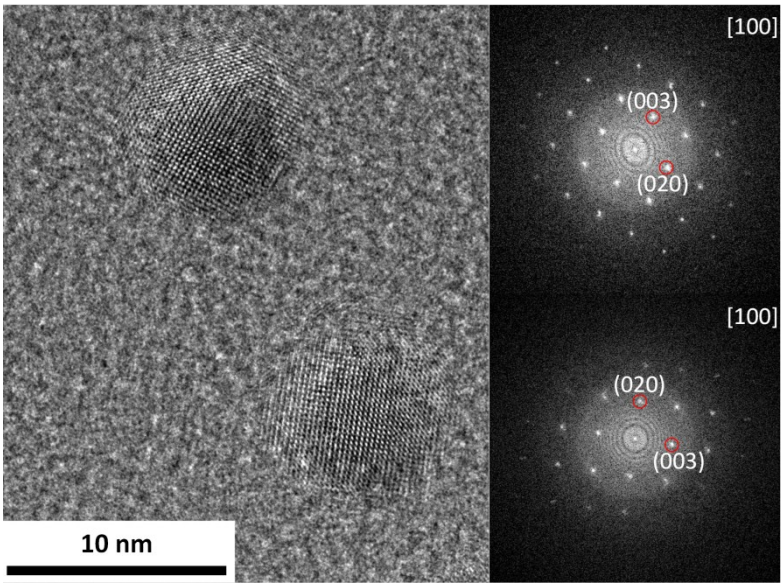

Figure S4. HRTEM of 5 % Eu^{3+}-doped LaOCl nanocrystals and corresponding Fourier transforms in insets. Intereticular planes and zone axes are indexed according to LaOCl structure in P4/nmm space group.

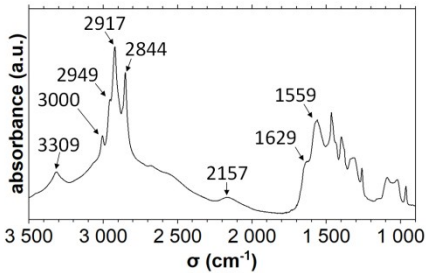

Figure S5. FTIR spectrum of Eu^{3+}-doped LaOCl nanocrystals showing bond vibrations typical of OLA, as opposed to OA.[7,8]

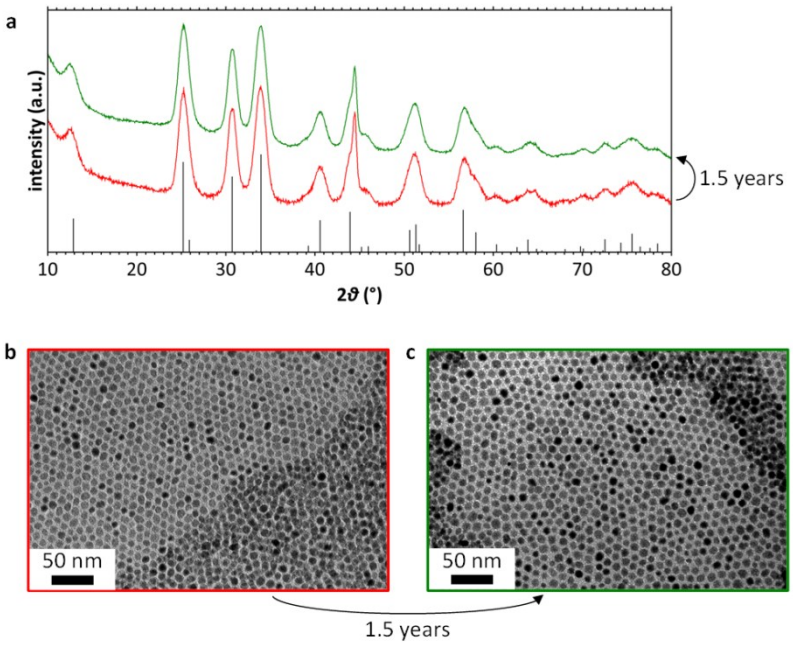

Figure S6. Stability of Eu^{3+}-doped LaOCl NCs before (red) and after (green) exposure to air at room temperature during 18 months. a) XRD diagrams performed on the same dried sample, b,c) TEM pictures obtained from the same grid.

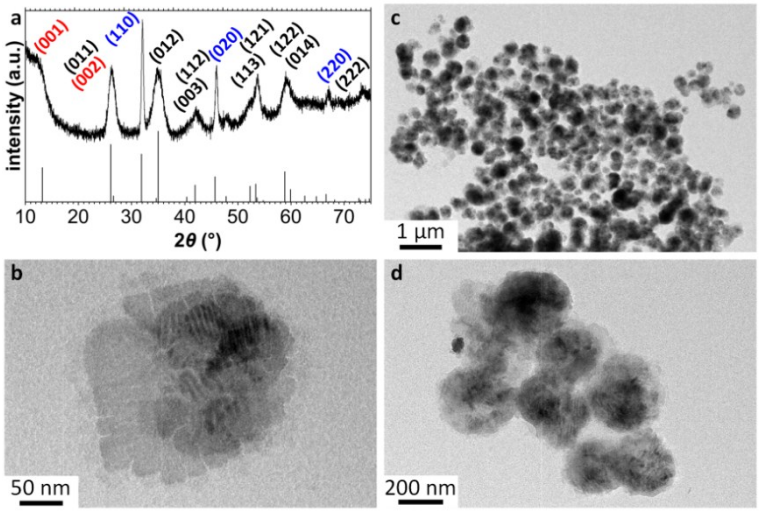

e

(hkl)	2ϑ (°)	ε_{hkl} (nm)
(001)	12.62	3.9
(011)	26.21	6.4
(002)	26.95	4.5
(110)	32.03	17.4
(012)	34.95	3.7
(020)	45.93	15.3
(220)	66.97	17.0

Figure S7. Structural characterization of GdOCl nanocrystals. The synthesis was adapted from LaOCl experiment, using hexahydrate gadolinium chloride as RE precursor, and without addition of OA at the end of the heating step. a) XRD diagram showed that GdOCl (P4/nmm, No. 129) is the only phase obtained. The various peak widths were due to strong shape anisotropy, in relation with crystalline structure. Especially, the narrowest peaks corresponded to (hk0) interreticular planes (blue), i.e. orthogonal to *c* axis. b-d) TEM pictures showed stacks of thin plates with rough edges, forming 200-500 nm spherical aggregates. e) Peak position and apparent crystal size (from Scherrer formula) of some interreticular planes (hkl). ε_{hk0} = 16.6±1.1 nm and ε_{00l} = 4.2±0.4 nm confirmed that GdOCl NCs were anisotropic with a smaller dimension in *c* direction, whereas facets orthogonal to *c* were the biggest. This is in agreement with the plate shape observed by TEM (b)).

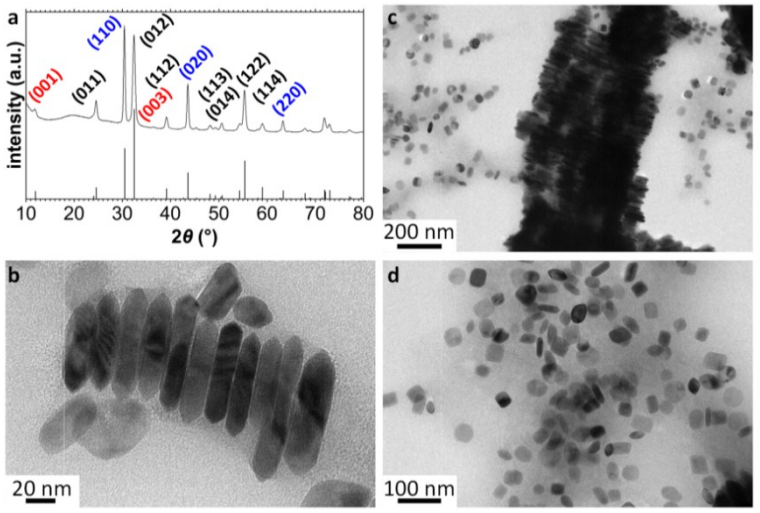

e

(hkl)	2ϑ (°)	ε_{hkl} (nm)
(001)	11.87	15.4
(110)	30.38	20.6
(012)	32.36	12.6
(003)	36.43	14.7
(112)	39.11	13.9
(013)	42.57	12.2
(020)	43.51	20.6
(021)	45.27	23.4
(113)	48.13	14.0
(014)	54.28	10.8
(122)	55.27	15.8
(023)	58.01	17.6
(114)	58.97	12.3
(220)	63.24	20.4

Figure S8. Structural characterization of LaOBr nanocrystals. The synthesis was adapted from LaOCl experiment, using lanthanum bromide instead of the chloride, heating at 330 °C instead of 220 °C, and without addition of OA at the end of the heating step. a) XRD diagram showed that LaOBr (P4/nmm, No. 129, ICSD code 84336) was the only phase obtained. b-d) TEM pictures of nanoplates 15-20 nm thick and 30-100 nm long. Particles displayed an elongated hexagon-like shape when oriented along the edge. This shape was similar than LaOCl obtained by Depner et al..[9] Rod-like arrays (single- and multi-linear) formed via face-to-face alignement of the nanoplates. e) Peak position and apparent crystal size (from Scherrer formula) of some interreticular planes (hkl). ε_{hk0} = 20.6±0.1 nm ε_{00l} = 15.1±0.5 nm confirmed that LaOBrl NCs are anisotropic with a smaller dimension in *c* direction, whereas the biggest facets were perpendicular to *c* axis. This was in agreement with the shape observed by TEM (b)). ε_{hk0} was smaller than plates length observed by TEM. The size difference could be due to tha nanoplates being polycrystalline.

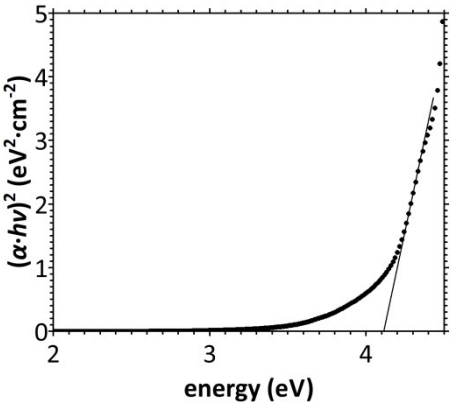

Figure S9. Tauc plot of dispersed LaOCl NCs.

For direct bandgap semiconductors such as LaOCl,[10] optical bandgap measurement was based on the Tauc relationship (2) between the absorption coefficient α, the photon energy $h\nu$ and the bandgap energy E_g:

$$\alpha\, h\nu = B\,(h\nu - E_g)^{1/2} \quad (2)$$

where B was a constant for allowed transitions. For relatively low absorption A (A < 1), the absorption coefficient of a perfectly non-scattering dispersion followed the linear Beer-Lambert law:

$$A = \alpha\, l \quad (3)$$

with l the optical path length (1 cm).

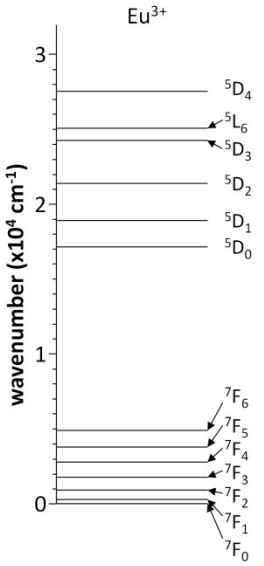

Figure S10. Partial energy diagram of Eu^{3+} ($4f^6$) taking into account interelectronic repulsion and spin-orbit coupling.[11]

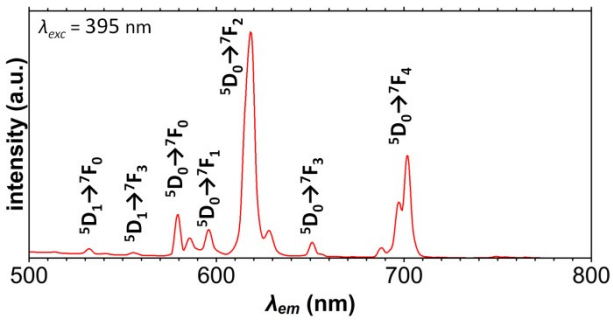

Figure S11. PL spectrum of Eu^{3+}-doped LaOCl NCs dispersed in chloroform, excitation at λ_{exc} = 395 nm. Slit bandwidths on both incident and emission sides were 3.0 nm.

REFERENCES

1 T. Roisnel and J. Rodríquez-Carvajal, *Mater. Sci. Forum*, 2001, **378–381**, 118–123.

2 J.-C. Boyer and F. C. J. M. van Veggel, *Nanoscale*, 2010, **2**, 1417.

3 C. Würth, M. Grabolle, J. Pauli, M. Spieles and U. Resch-Genger, *Nat. Protoc.*, 2013, **8**, 1535–1550.

4 M. Kaiser, C. Würth, M. Kraft, I. Hyppänen, T. Soukka and U. Resch-Genger, *Nanoscale*, 2017, **9**, 10051–10058.

5 C. Würth, S. Fischer, B. Grauel, A. P. Alivisatos and U. Resch-Genger, *J. Am. Chem. Soc.*, 2018, **140**, 4922–4928.

6 V. Petrícek, M. Dušek and L. Palatinus, *Zeitschrift fur Krist.*, 2014, **229**, 345–352.

7 S. Mourdikoudis and L. M. Liz-Marzán, *Chem. Mater.*, 2013, **25**, 1465–1476.

8 I. O. Perez De Berti, M. V Cagnoli, G. Pecchi, J. L. Alessandrini, S. J. Stewart, J. F. Bengoa and S. G. Marchetti, *Nanotechnology*, 2013, **24**, 175601.

9 S. W. Depner, K. R. Kort, C. Jaye, D. A. Fischer and S. Banerjee, *J. Phys. Chem. C*, 2009, **113**, 14126–14134.

10 L. Lv, T. Wang, S. Li, Y. Su and X. Wang, *CrystEngComm*, 2016, **18**, 907–916.

11 K. Binnemans, *Coord. Chem. Rev.*, 2015, **295**, 1–45.